NANO LETTERS

Letter

pubs.acs.org/NanoLett

Multiplexed Holograms by Surface Plasmon Propagation and Polarized Scattering

Ji Chen,[†,‡] Tao Li,*[,†,‡] Shuming Wang,*[,†,‡] and Shining Zhu[†,‡]

[†]National Laboratory of Solid State Microstructures, College of Engineering and Applied Sciences and [‡]Collaborative Innovation Center of Advanced Microstructures, Nanjing University, Nanjing 210093, China

Supporting Information

ABSTRACT: Thanks to the superiority in controlling the optical wave fronts, plasmonic nanostructures have led to various striking applications, among which metasurface holograms have been well developed and endowed with strong multiplexing capability. Here, we report a new design of multiplexed plasmonic hologram, which allows for reconstruction of multiple holographic images in free space by scatterings of surface plasmon polariton (SPP) waves in different propagation directions. Besides, the scattered polarization states can be further modulated by arranging the orientations of nanoscatterers. By incorporation of the SPP propagation and polarized scattering, a 4-fold hologram with low crosstalk is successfully demonstrated, which breaks the limitation of only two orthogonal states in conventional polarization multiplexers. Moreover, our design using the near-field SPP as reference wave holds the advantage for compact integration. This holographic approach is expected to inspire new photonic designs with enhanced information capacity and integratability.

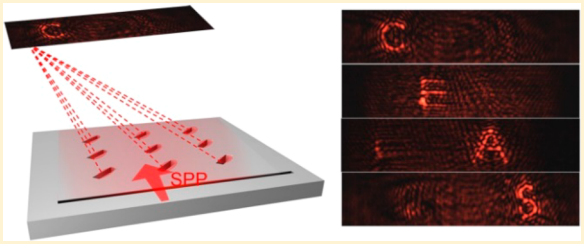

KEYWORDS: *Surface plasmon, holography, multiplexing, polarization*

The advances of artificial optical nanostructures have demonstrated the overwhelming capability in manipulating the phase, amplitude, and polarization of light in desirable manners.[1−3] Metasurface, as a 2D arrayed ultrathin structure with a reduced internal propagating loss compared with the bulk metamaterial, has attracted more attention recently, in which the unit cell resonance and geometric phase design were well developed as two major strategies in shaping the light wavefronts.[4−10] Up to now, many efforts were still ongoing toward the low-loss,[11−14] broadband,[15−19] and achromatic[20−23] optical functionalities. Among them, hologram with ultrasmall pixels and wide field of view is a promising application,[7,8,24−27] especially when multiple degrees of freedom of photon are involved for multiplexing[8,28−31] (e.g., polarizations, diffraction orders, focal planes). Compared with the conventional holograms, the metasurface provides people with a superb phase mask with enhanced imaging performance; however, the advantage of ultrathin thickness has not been used well. In principle, meta-devices would be of the high priority in compact integrations due to its subwavelength feature. Regarding a device of holographic imaging or display, if the illumination can be on-chip integrated without external optical source, it will greatly improve its device portability, stability, and extendibility, which would greatly promote the related researches to a more practical regime.

Surface plasmon polariton (SPP) is a bounded wave on metal surface with enhanced field and squeezed wavelength. Near-field holograms based on the SPP wave have been developed for the beam engineering in recent years.[32−35] In fact, the SPP wave also can work as the reference beam to generate a holographic image in the free space,[36−38] which possibly indicates a kind of compact on-chip display devices. As far as the multiplexing is concerned, how to engineer the SPP wave in holograms to record and display information as much as possible still remains an open question.

In this paper, we propose a new type of holographic multiplexing with multiple information recorded in a well arranged nanohole hologram, by which demultiplexed free-space images can be reconstructed under SPP illuminations with different propagation directions. It rightly takes the usage of the propagating SPP wave vectors that carry the phase information according to the holographic design. Four separated holographic images with respect to different propagating SPP excitations are demonstrated, and the crosstalk for more possible multiplexer is also discussed. Moreover, this holographic process is based on the scattering of the SPP wave to free space, where the shape of the hole scatterers is found to play an important role in controlling the imaging polarizations. By incorporating with the polarization, 4-fold hologram with almost zero crosstalk was realized by appropriate polarization control both in SPP excitation and imaging process. Such a hybrid holographic multiplexing reasonably breaks the limitation of only two orthogonal states in the polarization multiplexers and suggests new possibilities in future compact designs for versatile optical functionalities.

Received: May 31, 2017
Revised: July 4, 2017
Published: July 6, 2017

DOI: 10.1021/acs.nanolett.7b02295
Nano Lett. XXXX, XXX, XXX−XXX

According to the diffraction process of SPP wave to the free space, the propagating phase of SPP field can be selected out for scattering by introducing nanoscatterers at proper locations, by which optical Airy beams, polarized focusing beams, have been realized.[39,40] It is ready to extend such a diffraction/scattering process to the SPP involved holography, where the scattering structures (i.e., hologram) are designed by the interference of an SPP reference wave and the reversed diffraction wave from a certain spatial object. This hologram of constructive interference pattern on a metal surface can be retrieved from the equation of

$$\phi_{obj}(x, y) = \varphi_{spp}(x, y) + 2m\pi \quad (1)$$

where ϕ_{obj} is the phase distribution on metal plane required by the object, and φ_{spp} is phase of SPP reference wave. For an SPP wave with a wave vector $\vec{k}_{spp}$ propagating along $\vec{l}$, the phase evolution of it can be expressed as

$$\varphi_{spp} = \varphi_0 + \vec{k}_{spp} \cdot \vec{l} \quad (2)$$

From this equation it can be found that SPP waves propagating along different directions will possess different phase evolutions. Therefore, it would possibly provide people a new strategy to record multiple objects information into a single hologram pattern.

In experiment, the required phase distributions of reconstructed images are stored in a well-defined rectangle nanoscatterer array. By taking careful consideration on the fabrication precision, scattering intensity, and some testing results, suitable structural parameters of the scatterers were determined. All the rectangular-hole scatterers were of 300 nm in length, 100 nm in width, and 80 nm in depth, which were fabricated by focus ion beam (FIB dual-beam FEI Helios 600i) on a 200 nm thick silver film with a silica substrate. A slit with length of 30 μm besides the hologram structures was introduced to couple the incident He−Ne laser (λ_0 = 632.8 nm) to in-plane propagating SPP. When the SPP wave propagates through the nanoscatterings, it will be both diffracted out as radiation light and still confined on the metal surface as diffracted SPP waves. The diffracted out SPP will reconstruct images in space, which can be characterized by a microscope system with an objective of NA = 1.42.

According to the stated methods above, in the reconstruction process only a proper SPP wave with the right propagation direction can be diffracted to reconstruct the designed object. Such a reconstruction cannot be fulfilled by other directional SPPs for their unsatisfied phase evolutions. Taking the focusing case for example, the hologram can be obtained by the interference of a spherical wave from a point source and an SPP wave propagating along $-y$ direction, which corresponds to a reference SPP propagating in y-direction in the reconstruction process, as shown in Figure 1a. The red curve in the figure displays the phase distribution of the spherical wave along the y-axis, while the blue sawtooth shape line displays the phase evolution of the SPP wave. Their intersections determine the right positions of the scatterers, by which the hologram pattern is formed. When we excited the SPP in y-direction, a free-space spherical wave can be reconstructed by SPP scattering, which rightly gives rise to a focusing spot, as shown in Figure 1d. However, for an x-directional SPP wave, the phase is uniform that cannot be selected out for a focusing but a plane diffraction wave (see Figure 1b). As for the SPP wave propagating along $-y$ direction, the phase profile will be opposite and leads to an antifocusing (see Figure 1c). Unlike the focusing case, both the diffracted plane wave and an antifocusing wave will diffuse rapidly in the free space. Therefore, the intensity of their reconstructed field in the image plane (focal plane of the first case) will be much weaker compared with the focusing one, as shown in Figure 1e,f (Figure 1g shows their field intensity with ×10 enhancement). Note that Figure 1d−g are the calculation results by the diffraction theory with respect to hologram structures under different SPP excitations.

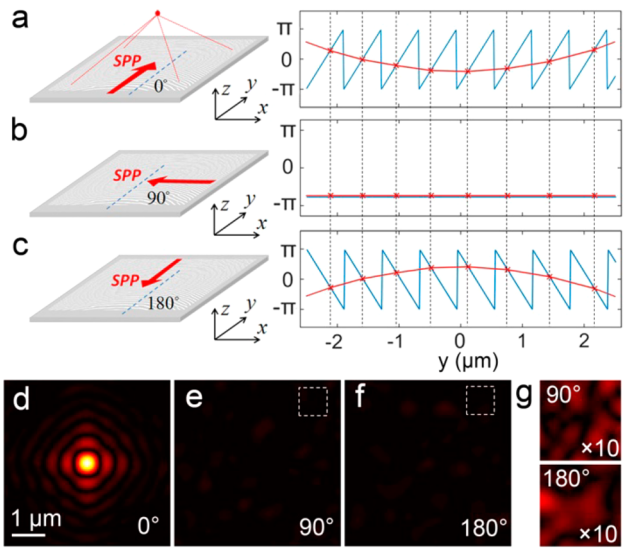

Figure 1. Influence of SPP propagation direction on holographic reconstruction. The scheme of SPP propagating through a hologram for (a) 0°, (b) 90°, and (c) 180° with respect to y-axis and the corresponding phases of them. The blue lines are the SPP phase evolutions on metal surface; the horizontal coordinates of red markers represent the positions of hologram pattern; and the red lines represent the phase of the required diffracting wave. The reconstructed field intensities under (d) 0°, (e) 90°, and (f) 180° conditions and (g) the zoom-in image of part of 90° and 180° cases with ×10 enhancement for observation.

From above analyses, we would possibly find a new way to multiplex multiple objects into a single hologram structure on a metal surface, which can be read out by different directional propagating SPPs. In this case, there will be multiple holograms overlapped that result in a number of sharing scatterers. To achieve the multiplexed hologram structure, one needs to carefully design the scatterers that can share how many target objects in reconstruction. If the scatterers shared too many targets, they must be reduced in number, which lowers the holographic efficiency and the image intensity. On the contrary, if the sharing is too small it is inevitable to produce crosstalk that is harmful for demultiplexing.

To demonstrate this strategy, we designed a multiplexed hologram with four objects of arrow-shaped points in different directions at 40 μm above the metal plane. According to aforementioned discussions, we first generated four hologram patterns with respect to four target images according to four directional SPPs excitations. Next, 4-fold and 3-fold crossings from the overlapped patterns are selected out for the multiplexing hologram (see Supporting Information (SI) Note 1). This hologram structure with an array of nanohole scatterers was fabricated by the focus ion beam (FIB) milling on a silver surface, beside which four nanoslits were also fabricated to launch the SPPs (see the method for the

DOI: 10.1021/acs.nanolett.7b02295
Nano Lett. XXXX, XXX, XXX−XXX

experimental details). Figure 2a shows the scanning electric microscope (SEM) image of our hologram sample. Here, we

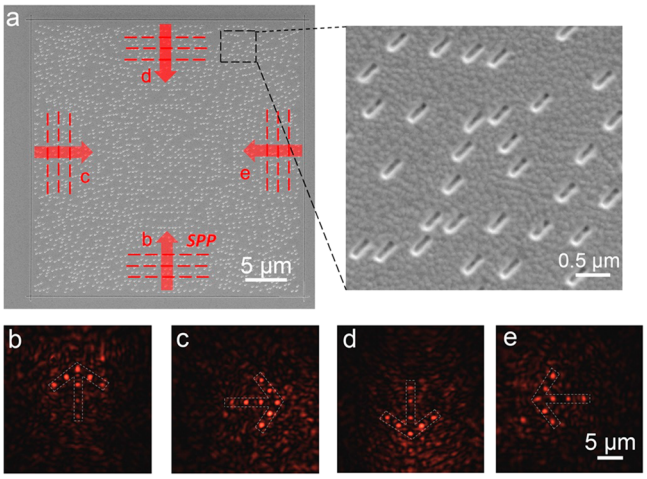

Figure 2. Design of 4-fold hologram multiplexed by propagating SPPs. (a) The SEM image of the 4-fold plasmonic hologram, in which the inset figure is the zoom-in image showing the details of hologram units. The letters beside the arrows label the correspondence of reconstructed images in panels b−e and the different directional SPP excitations. (b-e) The experimentally reconstructed holographic images with arrow-shaped points in different directions.

used rectangle holes as the scattering units with a uniform 45° orientation (as shown in the zoom-in SEM image in Figure 2a), which will reconstruct image with a certain linear polarization (it will be discussed later). Then, we can filter out the noisy background with different polarizations for a better observation. The experimental results of holographic images are shown in Figure 2b−e, where each orientated arrow image composed of eight points corresponds to each directional SPP excitation (marked as red arrows in Figure 2a). Although there are still some background noises, these four images are clearly manifested with almost no crosstalk, which indicates the capability for multiplexing four orthogonal states more than only two states in the polarization multiplexer.

In this multiplexed hologram, four reference SPPs are set with a step of 90° in propagation direction. One would further wonder how much information it can multiplex. To answer this question, a smallest angle between two SPPs' directions needs to find by which two holographic images should have low crosstalk. Then additional experiments with respect to different propagating angles were performed. It is shown that a deviation angle ≥20° can decrease the crosstalk to smaller than 0.1, which indicates about 18 independent channels can be used in such multiplexed hologram (more details are provided in SI Note 2).

In the scattering process, the SPP wave propagating through the rectangular hole will lead to charge accumulations mainly at two long sides of hole, which indeed acts as a oscillating dipole diffracting to the free space with polarization orthogonal to the hole long side (see the schematic image Figure S3a in SI Note 3). Therefore, it is ready to generate polarization controlled diffractions with respect to well-designed hole orientations. A simplest case is to generate a uniform linear polarization in the holographic reconstruction. In the experiment of Figure 2, we rightly take the usage of this property by arranging the 45° orientations for all nanoholes, which gives rise to four linear polarized images in −45° (Figure 2b−e). Such a polarized holography is useful to improve the image quality by filtering out the background noises with a proper polarizer in analyses.

Figure 3a schematically shows this polarized scattering process, inside which the uniform hole sample (left-inset)

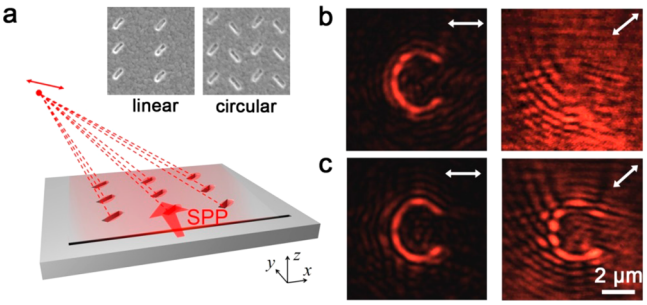

Figure 3. Design of polarization controlled holography. (a) Scheme of hologram with polarized diffracted units. The insets are the samples for linear (left) and circular (right) polarization. Reconstructed images corresponding to (b) linear polarization (−45°) and (c) circular polarization analyzed in different polarization states. In (b,c) the arrows at the top-right corners indicate the states of polarization analyzer.

corresponds to a linear holographic image of capital letter "C" with −45° polarization (i.e., the image disappears when checked in 45° polarization as shown in Figure 3b). The image is recorded in the plane of 40 μm distance to the sample, as well as the result in Figure 2. This method can be further used to generate holographic images with arbitrary polarizations more than the linear case. The right inset of Figure 3a displays another sample containing two sets of units with a cross angle of 90°. Under the excitation of a y-directional SPP wave, the near field will be diffracted out with two orthogonal linear polarized waves in a phase difference of $\Delta\varphi$. This $\Delta\varphi$ can be tuned by setting the relative displacement of two sublattices according the different SPP phase accumulations. As a result, arbitrary polarizations can be realized by superposing of these two orthogonal waves in diffraction with different $\Delta\varphi$, which can be expressed as

$$\Delta\varphi = (k_0 R_a + k_{spp} y_a) - (k_0 R_b + k_{spp} y_b) \quad (3)$$

where, k_0 is the wave vector of scattering wave in free space, k_{spp} is the wave vector of surface plasmon wave, R_a and R_b are the distances of image points to two orthogonal units respectively, y_a and y_b are the y-coordinate locations of these two units. For example, by setting $\Delta\varphi = \pm\pi/2$ as the case shown in the right inset of Figure 3a, circular polarized images can be obtained, as shown in Figure 3c. It can be seen that the "C" remains a strong intensity both in 0° and 45° polarization states in analyses, agreeing with the property of a circular polarization. In fact, holographic images with all kinds of polarization states in the Poincare sphere can be achieved by this means. More details can be found in SI Note 3.

According to above approaches, a 4-fold multiplexed hologram can be designed by incorporating the SPP propagation with polarized scattering, where only two directional propagating SPP are needed. Figure 4a displays our experimental sample with two zoom-in inset images showing the unit cells. It is found the left and right sides are responsible for two orthogonal polarizations (45° and −45°). A horizontal slit in the bottom and a vertical slit in the center (indicated by dashed lines) are also fabricated to launch the SPPs. Then these

DOI: 10.1021/acs.nanolett.7b02295
Nano Lett. XXXX, XXX, XXX−XXX

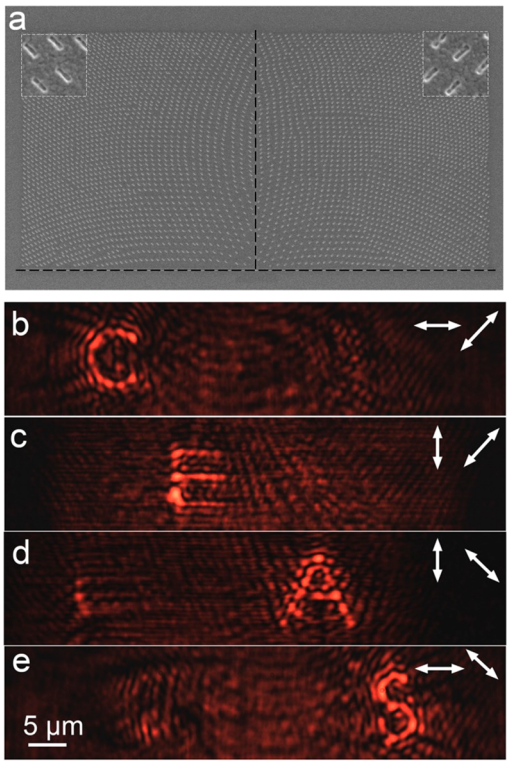

Figure 4. The 4-fold multiplexed hologram by SPP propagation and polarizer. (a) The multiplexed hologram is composed of two parts that are consist of diffracted units with $\alpha = 45°$ and $-45°$, respectively. The black dashed lines represent the position of slit couplers to launch the SPP. (b–e) Experimental results of four orthogonal images decoded from the multiplexed hologram according to different excitation and analyzer conditions. The first white arrow at the up-right corner represent the polarization of incident lights, and the second arrow represent the direction of analyzer polarization.

two orthogonally propagating SPPs are used to generate the multiplexed hologram, in which the orientated units are located at the intersections of two overlapped hologram patterns. In our design, both sides of the hologram attribute to two orthogonal states according to two different SPP excitations. Meanwhile, the scattering fields as the holographic reconstructions are still perpendicular to each other in polarizations. It means we can realize four isolated holographic images by carefully tuning the input SPP excitation and polarized analyzer. Because the SPP propagation can also be tuned by incident polarization with respect to two slit couplers, four images can be decoded from the 4-fold hologram by tuning the polarizers in front of and behind the hologram sample. To experimentally demonstrate this approach, a multiplexed hologram encoding phase information on capital letter "CEAS" is designed, with "CE" encoded at the left side and "AS" at the right side. Horizontally propagating SPP waves launched by *x*-polarized incidence is designed to reconstruct images of "C" and "S", while the *y*-propagating SPPs contribute to the images of "E" and "A". Figure 4b–e shows the experimental results of the demultiplexed four holographic images at an image plane of 40 μm, inside which the polarization states of excitation and analyzer are marked out in the top-right corners. From the figures, four capital letters can be clearly observed with good holographic imaging quality and almost no crosstalk.

In summary, we proposed and demonstrated a brand new approach to generate multiplexed holograms with respect of different propagating SPP waves as the references. By utilizing polarized diffractions with certain scatterer orientations, object waves with arbitrary polarizations were realized, which not only helps to improve the holographic imaging quality but also to realize a hybrid hologram for multiplexing more orthogonal states. We finally demonstrated a 4-fold hologram with good image quality and low crosstalk. Because the propagating SPP multiplexer possesses more channels, which enhance the capacity of plasmonic multiplexing, it offers people more flexible designs and new exciting possibility in optical information processing.

■ ASSOCIATED CONTENT

Supporting Information

The Supporting Information is available free of charge on the ACS Publications website at DOI: 10.1021/acs.nanolett.7b02295.

Design of multiplexed hologram, analyses of crosstalk, and reconstruction of images with arbitrary polarizations (PDF)

■ AUTHOR INFORMATION

Corresponding Authors

*E-mail: taoli@nju.edu.cn. URL: http://dsl.nju.edu.cn/litao/.
*E-mail: wangshuming@nju.edu.cn.

ORCID

Tao Li: 0000-0003-0049-471X

Author Contributions

T.L. supervised the research. T.L., J.C., and S.W. conceived the idea and designed the experiments. J.C. performed the numerical calculations, fabricated the sample, and performed the optical analyses with the assistance from S.W. T.L. and J.C. analyzed the results and wrote the paper. All authors contributed to the discussions.

Notes

The authors declare no competing financial interest.

■ ACKNOWLEDGMENTS

This work is supported by National Key Research and Development Program of China (2017YFA0303700, 2016YFA0202103), National Natural Science Foundation of China (Nos. 11674167, 11621091, 11322439), and PAPD from Jiangsu Province. T.L. thanks the support from Dengfeng Project B of Nanjing University.

■ REFERENCES

(1) Liu, N.; Guo, H.; Fu, L.; Kaiser, S.; Schweizer, H.; Giessen, H. *Nat. Mater.* **2008**, *7*, 31–37.
(2) Soukoulis, C. M.; Wegener, M. *Nat. Photonics* **2011**, *5*, 523–530.
(3) Zheludev, N. I.; Kivshar, Y. S. *Nat. Mater.* **2012**, *11*, 917–924.
(4) Yu, N.; Genevet, P.; Kats, M. A.; Aieta, F.; Tetienne, J.-P.; Capasso, F.; Gaburro, Z. *Science* **2011**, *334*, 333–337.
(5) Sun, S.; He, Q.; Xiao, S.; Xu, Q.; Li, Q.; Zhou, L. *Nat. Mater.* **2012**, *11*, 426–431.
(6) Kildishev, A. V.; Boltasseva, A.; Shalaev, V. M. *Science* **2013**, *339*, 1232009.
(7) Montelongo, Y.; Tenorio-Pearl, J. O.; Williams, C.; Zhang, S.; Milne, W. I.; Wilkinson, T. D. *Proc. Natl. Acad. Sci. U. S. A.* **2014**, *111*, 12679–12683.
(8) Chen, W. T.; Yang, K.-Y.; Wang, C.-M.; Huang, Y.-W.; Sun, G.; Chiang, I.-D.; Liao, C. Y.; Hsu, W. L.; Lin, H. T.; Sun, S.; Zhou, L.; Liu, A. Q.; Tsai, D. P. *Nano Lett.* **2014**, *14*, 225–230.

DOI: 10.1021/acs.nanolett.7b02295
Nano Lett. XXXX, XXX, XXX–XXX

(9) Huang, L.; Chen, X.; Mühlenbernd, H.; Li, G.; Bai, B.; Tan, Q.; Jin, G.; Zentgraf, T.; Zhang, S. *Nano Lett.* **2012**, *12*, 5750−5755.
(10) Chen, X.; Huang, L.; Mühlenbernd, H.; Li, G.; Bai, B.; Tan, Q.; Jin, G.; Qiu, C.-W.; Zhang, S.; Zentgraf, T. *Nat. Commun.* **2012**, *3*, 1198.
(11) Pfeiffer, C.; Grbic, A. *Phys. Rev. Lett.* **2013**, *110* (19), 197401.
(12) Jiang, Z. H.; Yun, S.; Lin, L.; Bossard, J. A.; Werner, D. H.; Mayer, T. S. *Sci. Rep.* **2013**, *3*, 1571.
(13) Monticone, F.; Estakhri, N. M.; Alù, A. *Phys. Rev. Lett.* **2013**, *110*, 203903.
(14) Decker, M.; Staude, I.; Falkner, M.; Dominguez, J.; Neshev, D. N.; Brener, I.; Pertsch, T.; Kivshar, Y. S. *Adv. Opt. Mater.* **2015**, *3*, 813−820.
(15) Sun, S.; Yang, K.-Y.; Wang, C.-M.; Juan, T.-K.; Chen, W. T.; Liao, C. Y.; He, Q.; Xiao, S.; Kung, W. T.; Guo, G.-Y.; Zhou, L.; Tsai, D. P. *Nano Lett.* **2012**, *12*, 6223−6229.
(16) Gansel, J. K.; Thiel, M.; Rill, M. S.; Decker, M.; Bade, K.; Saile, V.; von Freymann, G.; Linden, S.; Wegener, M. *Science* **2009**, *325*, 1513−1515.
(17) Ni, X.; Emani, N. K.; Kildishev, A. V.; Boltasseva, A.; Shalaev, V. M. *Science* **2012**, *335*, 427.
(18) Yu, N.; Aieta, F.; Genevet, P.; Kats, M. A.; Gaburro, Z.; Capasso, F. *Nano Lett.* **2012**, *12*, 6328−6333.
(19) Li, X.; Chen, L.; Li, Y.; Zhang, X.; Pu, M.; Zhao, Z.; Ma, X.; Wang, Y.; Hong, M.; Luo, X. *Sci. Adv.* **2016**, *2*, e1601102.
(20) Khorasaninejad, M.; Aieta, F.; Kanhaiya, P.; Kats, M. A.; Genevet, P.; Rousso, D.; Capasso, F. *Nano Lett.* **2015**, *15*, 5358−5362.
(21) Aieta, F.; Kats, M. A.; Genevet, P.; Capasso, F. *Science* **2015**, *347* (6228), 1342−1345.
(22) Arbabi, A.; Arbabi, E.; Kamali, S. M.; Horie, Y.; Han, S.; Faraon, A. *Nat. Commun.* **2016**, *7*, 13682.
(23) Khorasaninejad, M.; Zhu, A. Y.; Roques-Carmes, C.; Chen, W. T.; Oh, J.; Mishra, I.; Devlin, R. C.; Capasso, F. *Nano Lett.* **2016**, *16*, 7229−7234.
(24) Ni, X.; Kildishev, A. V.; Shalaev, V. M. *Nat. Commun.* **2013**, *4*, 2807.
(25) Huang, L.; Chen, X.; Mühlenbernd, H.; Zhang, H.; Chen, S.; Bai, B.; Tan, Q.; Jin, G.; Cheah, K.-W.; Qiu, C.-W.; Li, J.; Zentgraf, T.; Zhang, S. *Nat. Commun.* **2013**, *4*, 2808.
(26) Huang, Y.-W.; Chen, W. T.; Tsai, W.-Y.; Wu, P. C.; Wang, C.-M.; Sun, G.; Tsai, D. P. *Nano Lett.* **2015**, *15*, 3122−3127.
(27) Zheng, G.; Mühlenbernd, H.; Kenney, M.; Li, G.; Zentgraf, T.; Zhang, S. *Nat. Nanotechnol.* **2015**, *10*, 308−312.
(28) Huang, L.; Mühlenbernd, H.; Li, X.; Song, X.; Bai, B.; Wang, Y.; Zentgraf, T. *Adv. Mater.* **2015**, *27*, 6444−6449.
(29) Wen, D.; Yue, F.; Li, G.; Zheng, G.; Chan, K.; Chen, S.; Chen, M.; Li, K. F.; Wong, P. W.; Cheah, K. W.; Pun, E. Y.; Zhang, S.; Chen, X. *Nat. Commun.* **2015**, *6*, 8241.
(30) Ye, W.; Zeuner, F.; Li, X.; Reineke, B.; He, S.; Qiu, C.-W.; Liu, J.; Wang, Y.; Zhang, S.; Zentgraf, T. *Nat. Commun.* **2016**, *7*, 11930.
(31) Malek, S. C.; Ee, H.-S.; Agarwal, R. *Nano Lett.* **2017**, *17*, 3641−3645.
(32) Epstein, I.; Arie, A. *Phys. Rev. Lett.* **2014**, *112*, 023903.
(33) Libster-Hershko, A.; Epstein, I.; Arie, A. *Phys. Rev. Lett.* **2014**, *113*, 123902.
(34) Epstein, I.; Lilach, Y.; Arie, A. *J. Opt. Soc. Am. B* **2014**, *31*, 1642−1647.
(35) Chen, J.; Li, L.; Li, T.; Zhu, S. N. *Sci. Rep.* **2016**, *6*, 28926.
(36) Ozaki, M.; Kato, J.-I.; Kawata, S. *Science* **2011**, *332*, 218−220.
(37) Dolev, I.; Epstein, I.; Arie, A. *Phys. Rev. Lett.* **2012**, *109*, 203903.
(38) Chen, Y. H.; Huang, L.; Gan, L.; Li, Z. Y. *Light: Sci. Appl.* **2012**, *1*, e26.
(39) Tang, X. M.; Li, L.; Li, T.; Wang, Q. J.; Zhang, X. J.; Zhu, S. N.; Zhu, Y. Y. *Opt. Lett.* **2013**, *38*, 1733−1735.
(40) Li, L.; Li, T.; Tang, X. M.; Wang, S. M.; Wang, Q. J.; Zhu, S. N. *Light: Sci. Appl.* **2015**, *4*, e330.

DOI: 10.1021/acs.nanolett.7b02295
Nano Lett. XXXX, XXX, XXX−XXX